



***ab initio* Thermodynamic Study of the CO₂ Capture Properties of M₂CO₃ (M = Na, K)- and CaCO₃-Promoted MgO Sorbents Towards Forming Double Salts**

Yuhua Duan^{1*}, Keling Zhang², Xiaohong S. Li², David L. King², Bingyun Li^{1,3}, Lifeng Zhao⁴, Yunhan Xiao⁴

¹ National Energy Technology Laboratory, United States Department of Energy, 236 Cochran Mill Road, Pittsburgh, Pennsylvania 15236, USA

² Institute for Integrated Catalysis, Pacific Northwest National Laboratory, P. O. Box 999, Richland, WA 99354, USA

³ School of Medicine, West Virginia University, Morgantown, West Virginia 26506, USA

⁴ Key Laboratory of Advanced Energy and Power, Institute of Engineering Thermophysics, Chinese Academy of Sciences, P. O. Box 2706, Beijing 100190, China

ABSTRACT

The CO₂ capture properties of M₂CO₃ (M = Na, K)-promoted and CaCO₃-promoted MgO sorbents are investigated by first-principles density functional theory complemented with lattice phonon calculations. The calculated thermodynamic properties indicate that by forming double salts (M₂Mg(CO₃)₂ and CaMg(CO₃)₂), compared to pure MgO, the maximum allowable CO₂ capture temperatures of the M₂CO₃- and CaCO₃- modified MgO sorbents are shifted to higher temperature ranges. Under pre-combustion conditions with P_{CO₂} = 10 bar, the Na₂CO₃-promoted and CaCO₃-promoted MgO sorbents can capture CO₂ at temperatures as high as 915 K and 740 K respectively. While under post-combustion conditions with P_{CO₂} = 0.1 bar, their maximum allowable CO₂ capture temperatures are 710 K and 600 K respectively. However, when adding K₂CO₃ into MgO, under both pre- and post-combustion conditions, its maximum CO₂ capture temperatures only increased about 10 K relative to pure MgO. These results indicate that by mixing another solid into MgO, it is possible to shift its CO₂ capture temperature to fit practical industrial needs.

Keywords: CO₂ capture sorbents; Double salt sorbents; Density functional theory; Lattice phonon dynamics; Thermodynamics.

INTRODUCTION

Carbon dioxide (CO₂) from large stationary sources such as power plants has been identified as one of the leading causes of global warming (White *et al.*, 2003; Allen *et al.*, 2009). Carbon-free or carbon-neutral renewable energy sources are not likely to completely replace fossil fuel power plants for many years to come (Lund and Mathiesen, 2009). Hence, there is a need to reduce CO₂ emission by carbon capture and sequestration so that fossil fuel power plants may be operated without releasing enormous quantities of CO₂ into the atmosphere (Haszeldine, 2009; MacDowell *et al.*, 2010; Markewitz *et al.*, 2012; Li *et al.*, 2013). Accordingly, solid sorbent materials have been proposed for capture of CO₂ through a reversible chemical transformation. Among them, alkali and alkaline metal oxide based solid sorbents can play an important role for CO₂ capture as

they can be used over a wide temperature range (Stamnore and Gilot, 2005; Lee *et al.*, 2006; Lee and Kim, 2007; Siriwardane *et al.*, 2007; Lee *et al.*, 2008; Duan and Sorescu, 2009, 2010; Duan *et al.*, 2011).

CaO and MgO have been widely studied as CO₂ sorbents due to their potential high CO₂ capacity and low material cost (Wang *et al.*, 2011). Having high reactivity with CO₂, CaO can be used as a CO₂ sorbent in post-combustion technology as it can capture CO₂ with a carbonation/calcination looping cycle at high temperature (Yang *et al.*, 2010), while MgO can be used in pre-combustion CO₂ capture technology (Hassanzadeh and Abbasian, 2010; Abbasi *et al.*, 2013). However, although its theoretical CO₂ capture capacity (109 wt%) is very high, practically, the unmodified MgO has a very low CO₂ capacity of 0.24 mmol/g at 473 K (Zhang *et al.*, 2013). Improving its practical CO₂ capacity is the key issue in order to use MgO as CO₂ sorbent. Recent studies showed that when MgO was doped with alkali and alkaline metal carbonates, its CO₂ capture capacity increased and its maximum absorption temperature could be shifted (Mayorga *et al.*, 2001; Lee *et al.*, 2008; Montero *et al.*, 2010; Zhang *et al.*, 2013). For example, when Na₂CO₃ doped into MgO, the CO₂ capacity of the

* Corresponding author.

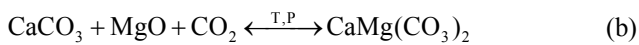
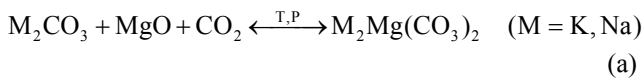
Tel.: 1-412-386-5771; Fax: 1-412-386-5990
E-mail address: yuhua.duan@netl.doe.gov

newly formed sorbent is 1–7 mmol CO₂/g depending on the temperature and dopant loading (Mayorga *et al.*, 2001). We did a further investigation on Na₂CO₃-promoted MgO sorbent and found that by forming Na₂Mg(CO₃)₂ double salt its operating temperature is increased to about 673 K which is compatible with warm gas cleanup (573–773 K) from a pre-combustion syngas (Zhang *et al.*, 2013). A similar double salt Cs₂Mg(CO₃)₂ was also observed in the Cs promoted triglyceride transesterification over MgO nanocatalysts (Montero *et al.*, 2010). The K₂CO₃-promoted MgO-based sorbent was investigated by several research groups (Lee *et al.*, 2006; Lee *et al.*, 2008; Xiao *et al.*, 2011). Their results showed that its CO₂ capture capacity could be as high as 197.6 mg CO₂/g, and after CO₂ absorption the double salts K₂Mg(CO₃)₂ and K₂Mg(CO₃)₂·4(H₂O) were formed. Li *et al.* investigated the dolomite modified with acetic acid for CO₂ capture and found that the calcined modified dolomite possesses greater surface area and pore volume than calcined original sorbent during the multiple cycles (Li *et al.*, 2008).

However, the thermodynamics and mechanisms of formation of these carbonate-promoted MgO sorbents still remain unclear. In this study, based on our computational methodology (Duan and Sorescu, 2009, 2010; Duan *et al.*, 2012), we first calculate the thermodynamic properties of the double salts (Na₂Mg(CO₃)₂, K₂Mg(CO₃)₂, and CaMg(CO₃)₂). Then based on the obtained data, we investigated the CO₂ capture properties of M₂CO₃ (M = Na, K)- and CaCO₃-promoted MgO sorbent systems.

COMPUTATIONAL METHODS

The complete description of our computational methodology can be found in our previous papers (Duan and Sorescu, 2009, 2010, 2011; Duan *et al.*, 2011). Here, we limit ourselves to provide only the main aspects relevant to the current study. When examining the M₂CO₃ (M = Na, K)- and CaCO₃-promoted MgO as CO₂ absorbents, we consider the following reactions:



Assuming the difference between the chemical potential of solid phases (M₂CO₃, CaCO₃, MgO, M₂Mg(CO₃)₂, and CaMg(CO₃)₂) can be approximated by the differences in their electronic energies (ΔE^{DFT}), entropies (ΔS_{PH}), and harmonic free energies (ΔF_{PH}), we can obtain the temperature and pressure dependent chemical potential (Δμ) for these reactions

$$\Delta\mu(T, P) = \Delta\mu^0(T) - RT \ln\left(\frac{P_{\text{CO}_2}}{P_0}\right) \quad (1)$$

with

$$\Delta\mu^0(T) = \Delta E^{\text{DFT}} + \Delta E_{\text{ZP}} + \Delta F_{\text{PH}}(T) - G_{\text{CO}_2}(T) \quad (2)$$

where ΔE_{ZP} is the zero point energy difference between the reactants and products, which can be obtained directly from phonon calculations. P₀ is the standard state reference pressure of 1 bar. The enthalpy change for the reactions (a) and (b), ΔH^{cal}(T), can be derived from the above equations as

$$\Delta H^{\text{cal}}(T) = \Delta\mu^0(T) + T(\Delta S_{\text{PH}}(T) - S_{\text{CO}_2}(T)) \quad (3)$$

As described in our previous study (Duan and Sorescu, 2009, 2010; Duan *et al.*, 2011, 2012), the zero-point energy, the free energy and the entropy of CO₂ (E_{ZP,CO2}, G_{CO2}(T), S_{CO2}(T)) can be obtained by standard statistical mechanics and accurately evaluated using the Shomate equation. In Eq. (2), ΔE^{DFT} is the total energy change of the reactants and products calculated by density functional theory (DFT). In this work, the Vienna *Ab-initio* Simulation Package (VASP) (Kresse and Hafner, 1993) was employed to calculate the electronic structures of the solid materials involved in this study. All calculations have been done using the projector augmented wave (PAW) pseudo-potentials and the PW91 exchange-correlation functional (Perdew and Wang, 1992). This computational level was shown to provide an accurate description of oxide systems (Duan and Sorescu, 2010; Duan, 2011; Duan *et al.*, 2011). Plane wave basis sets were used with a cutoff energy of 500 eV and a kinetic energy cutoff for augmentation charges of 605.4 eV. The k-point sampling grids of n₁ × n₂ × n₃, obtained using the Monkhorst-Pack method (Monkhorst and Pack, 1976), were used for these bulk calculations, where n₁, n₂, and n₃ were determined consistent to a spacing of about 0.028 Å⁻¹ along the axes of the reciprocal unit cells. The corresponding k-points sets that we used in our calculations were 8 × 8 × 2 for Na₂Mg(CO₃)₂ and K₂Mg(CO₃)₂, and 9 × 9 × 2 for CaMg(CO₃)₂, respectively. During the calculations, all atoms in the cell as well as the lattice dimensions and angles were relaxed to the equilibrium configurations.

In Eqs. (2) and (3), the zero-point-energies (E_{ZP}), entropies (S_{PH}), and harmonic free energies (F_{PH}, excluding zero-point energy which was already counted into the term ΔE_{ZP}) of solids were calculated by the PHONON software package (Parlinski, 2010) in which the direct method is applied following the formula derived by Parlinski *et al.* (1997) to combine *ab initio* DFT with lattice phonon dynamics calculations. In the phonon calculations, a 3 × 3 × 1 supercell is created for Na₂Mg(CO₃)₂, K₂Mg(CO₃)₂, and CaMg(CO₃)₂ from their optimized unit cells that are calculated through DFT for phonon calculations. Based on the partition function carried out with the phonon dispersions and phonon densities of states, their thermodynamic properties, such as internal energy, free energy, entropy, heat capacity, etc., can be evaluated under different temperature and pressure. These values are used in Eq. (1) to calculate the chemical potentials for the reactions (a) and (b). The available experimental thermodynamic data were taken from HSC

Chemistry package (www.outotec.com/hsc) and FactSage package (www.factsage.com).

RESULTS AND DISCUSSION

DFT and Phonon Calculated Results

Eitelite, $\text{Na}_2\text{Mg}(\text{CO}_3)_2$, has a hexagonal structure with space group $R\bar{3}H$ (#148) (Pabst, 1973). The structure of synthetic $\text{K}_2\text{Mg}(\text{CO}_3)_2$ is trigonal with space group $R\bar{3}mH$ (#166) which is isostructural with buetschliite, $\text{K}_2\text{Ca}(\text{CO}_3)_2$ (Hesse and Simons, 1982). Similar to $\text{Na}_2\text{Mg}(\text{CO}_3)_2$, the structure of dolomite, $\text{CaMg}(\text{CO}_3)_2$, is also a trigonal with space group $R\bar{3}H$ (#148) which can be described as a corner-linked structure of filled octahedral and nearly planar CO_3 groups (Reeder and Markgraf, 1986). Compared to calcite (CaCO_3), the lower symmetry of dolomite results from the alternating Ca and Mg layers and the slight rotation of the CO groups which move the oxygen atoms off the diad axes that exist in calcite. By applying this double salt crystal structural information into our modeling scheme,

the optimized lattice constants and total electronic energies of these three double salts as well as the corresponding carbonates and oxides considered in this work are presented in Table 1 (Duan and Sorescu, 2010; Duan *et al.*, 2011; Duan, 2012), along with experimental structural data. The agreement between the DFT optimized lattice constants and experimental data is generally very good. The calculated energy (E^{DFT}) for each solid is used to evaluate the DFT energy change (ΔE^{DFT} in Eq. (2)) of the CO_2 capture reactions (a) and (b).

Phonon calculations were performed for the double salts listed in Table 1. The finite temperature thermodynamic properties were then computed from the calculated phonon density of states by following our previous approach (Duan and Sorescu, 2010). The calculated phonon free energies, entropies, and heat capacities of these solid phase materials involved in this study are plotted as a function of temperature in Fig. 1. The zero-point energy (E_{ZP}) of each compound and corresponding available experimental measured data are also listed in Table 1.

Table 1. Comparison of the experimental and DFT calculated structural parameters and energies for the compounds in the reactions studied, with all distances in angstroms and angles in degrees. The zero-point energy and entropy calculated from phonon density of states, as well as the experimental data are also listed.

Compound	Space group	Structural parameters (Å, degree)		Calculated Energy (eV/f.u.)		Entropy (J/mol·K)	
		Experimental	Calculated	E^{DFT}	E_{ZP}	Calc. ($T = 300$ K)	Exp. ^a ($T = 298$ K)
MgO^b	$\text{Fm}\bar{3}m$ (No.225)	$a = 4.2198$	$a = 4.24888$	-12.00759	0.12611	33.29	26.95
$\text{Na}_2\text{Mg}(\text{CO}_3)_2$	$R\bar{3}H$ (No. 148)	$a = 4.942$ $c = 16.406$ $\gamma = 120^\circ$	$a = 4.97803$ $c = 16.50214$ $\gamma = 120^\circ$	-73.54023	1.03646	203.91	
$\text{K}_2\text{Mg}(\text{CO}_3)_2$	$R\bar{3}mH$ (No. 166)	$a = 5.150$ $c = 17.290$ $\gamma = 120^\circ$	$a = 5.21234$ $c = 17.76371$ $\gamma = 120^\circ$	-72.93267	0.99342	222.71	
$\text{CaMg}(\text{CO}_3)_2$	$R\bar{3}H$ (No. 148)	$a = 4.8069$ $c = 16.002$ $\gamma = 120^\circ$	$a = 4.85035$ $c = 16.10087$ $\gamma = 120^\circ$	-73.74471	1.02650	159.89	155.23 166.69
CaO^b	$\text{Fm}\bar{3}m$ (No. 225)	$a = 4.8152$	$a = 4.81903$	-12.98752	0.11088	39.37	38.10
Na_2O^b	$\text{Fm}\bar{3}m$ (No. 225)	$a = 5.55$	$a = 5.58517$	-11.34789	0.12801	76.84	75.04
K_2O^b	$\text{Fm}\bar{3}m$ (No. 225)	$a = 6.436$	$a = 6.52362$	-10.14413	0.08048	112.14	94.10
MgCO_3^b	$R\bar{3}cH$ (No. 167)	$a = 4.6338$ $c = 15.0192$ $\beta = 120^\circ$	$a = 4.68649$ $c = 15.13795$ $\beta = 120^\circ$	-35.96046	0.53235	69.35	65.09
CaCO_3^b	$R\bar{3}cH$ (No. 167)	$a = 4.991$ $c = 17.068$ $\beta = 120^\circ$	$a = 5.03979$ $c = 17.12672$ $\beta = 120^\circ$	-37.61011	0.48410	95.99	91.71
Na_2CO_3^b	$C12/m1$ (No. 12)	$a = 9.01029$ $b = 5.23116$ $c = 6.34548$ $\beta = 96.062^\circ$	$a = 8.95180$ $b = 5.33507$ $c = 6.13861$ $\beta = 102.21^\circ$	-37.29272	0.49152	122.53	138.78
K_2CO_3^b	$P12_1/c1$ (No. 14)	$a = 5.63961$ $b = 9.8312$ $c = 6.83407$ $\beta = 98.703^\circ$	$a = 5.76055$ $b = 9.90478$ $c = 7.18110$ $\beta = 97.30^\circ$	-36.90480	0.45733	160.12	155.50
CO_2 molecule	$P1$ ($D_{\infty h}$)	$r_{\text{C-O}} = 1.163$	$r_{\text{C-O}} = 1.1755$	-22.99409	0.31598		213.39

^a Taken from HSC Chemistry Package.

^b From references (Duan and Sorescu, 2010; Duan *et al.*, 2011; Duan, 2012).

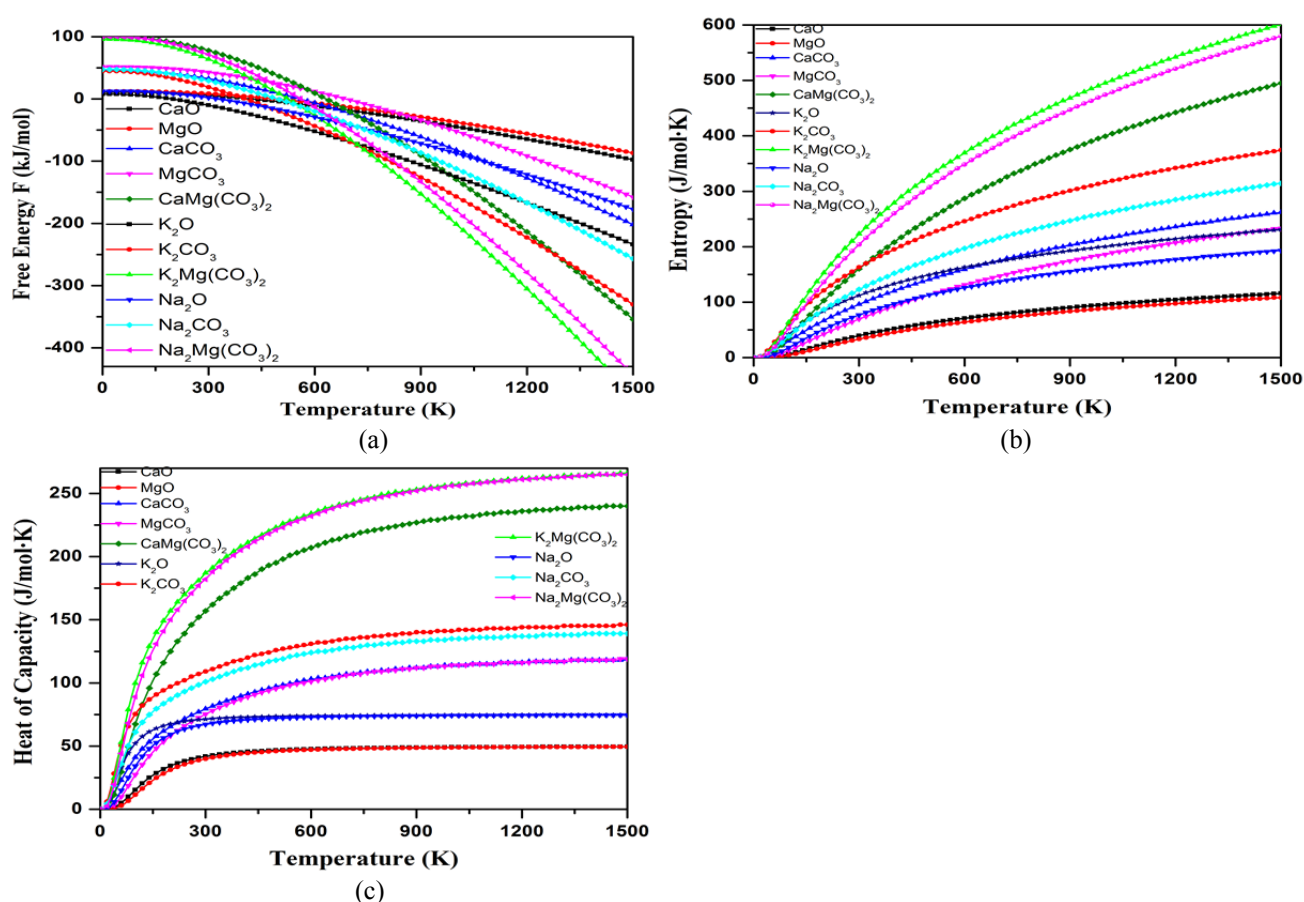


Fig. 1. Calculated (a) phonon free energies, (b) entropies and (c) heat of capacities for various solids studied as a function of temperature.

From Table 1, one can see that the calculated entropies of CaMg(CO₃)₂ and corresponding carbonates and oxides are in good agreement with the experimentally measured values. The calculated entropy of dolomite (159.89 J/mol·K) is between the two experimental values of 155.22 and 166.69 J/mol·K. Along with our previous studies on oxides and carbonates (Duan and Sorescu, 2010; Duan et al., 2011), these results indicate our theoretical approach can predict the reasonable thermodynamic properties of solids. As shown in Fig. 1, with increasing temperature, the free energy (F) of each solid is decreased while its entropy (S) and heat of capacity (C_p) is increased. At T = 0 K, the S and C_p of each solid is zero while its F = E_{zp}.

Thermodynamic Properties of the CO₂ Capture Reactions

By applying above calculated thermodynamic data into Eqs. (2) and (3) and setting the system pressure to 1 bar (in this case, $\Delta\mu^0$ in Eq. (2) is the same as Gibbs free energy change ΔG), we can obtain the thermodynamic properties of reactions (a) and (b) which are shown in Figs. 2 and 3 respectively. For systematic analysis, the calculated thermodynamic data of reactions of the corresponding oxides capturing CO₂ as well as the double salt formation from the carbonates are also plotted in Figs. 2 and 3. Table 2 summarizes these results. For comparison, the available experimental thermodynamic data of the CO₂ capture

reactions by MgO and dolomite are also shown in Figs. 2 and 3 as well as listed in Table 2.

As shown in Table 2, overall, the calculated ΔH and ΔG of these reactions are in good agreement with the available experimental data. The zero-point energy changes (ΔE^{zp}) of the CO₂ capture reactions are significant and should be included into their thermodynamic analysis. For the double salt formation reactions $M_2CO_3 + MgCO_3 = M_2Mg(CO_3)_2$ (M = Na, K) and $CaCO_3 + MgCO_3 = CaMg(CO_3)_2$, their ΔE^{zp} are much smaller (< 2 kJ/mol) and negligible. Within the temperature range 300 K–1500 K, their ΔH and ΔG are negative which means these the double salts are stable and can be formed by two single carbonates. At room temperature, Na₂Mg(CO₃)₂ is more stable than dolomite and K₂Mg(CO₃)₂.

From Fig. 2(a) it can be noticed that, for reaction $MgO + CO_2 = MgCO_3$, its experimental heat of reaction (ΔH) from the HSC Chemistry and FactSage databases have about a 20 kJ/mol discrepancy. Our calculated results are between these two sets of experimental values, but align closer to the HSC Chemistry values. The discontinuity of ΔH from HSC data at around 1300 K indicates there is a phase change. In the calculated the temperature range, the ΔH of reaction $MgO + CO_2 + Na_2CO_3 = Na_2Mg(CO_3)_2$ is lower than that of $MgO + CO_2 = MgCO_3$ but higher than that of $Na_2O + CO_2 = Na_2CO_3$. Similar trends were also found in dolomite

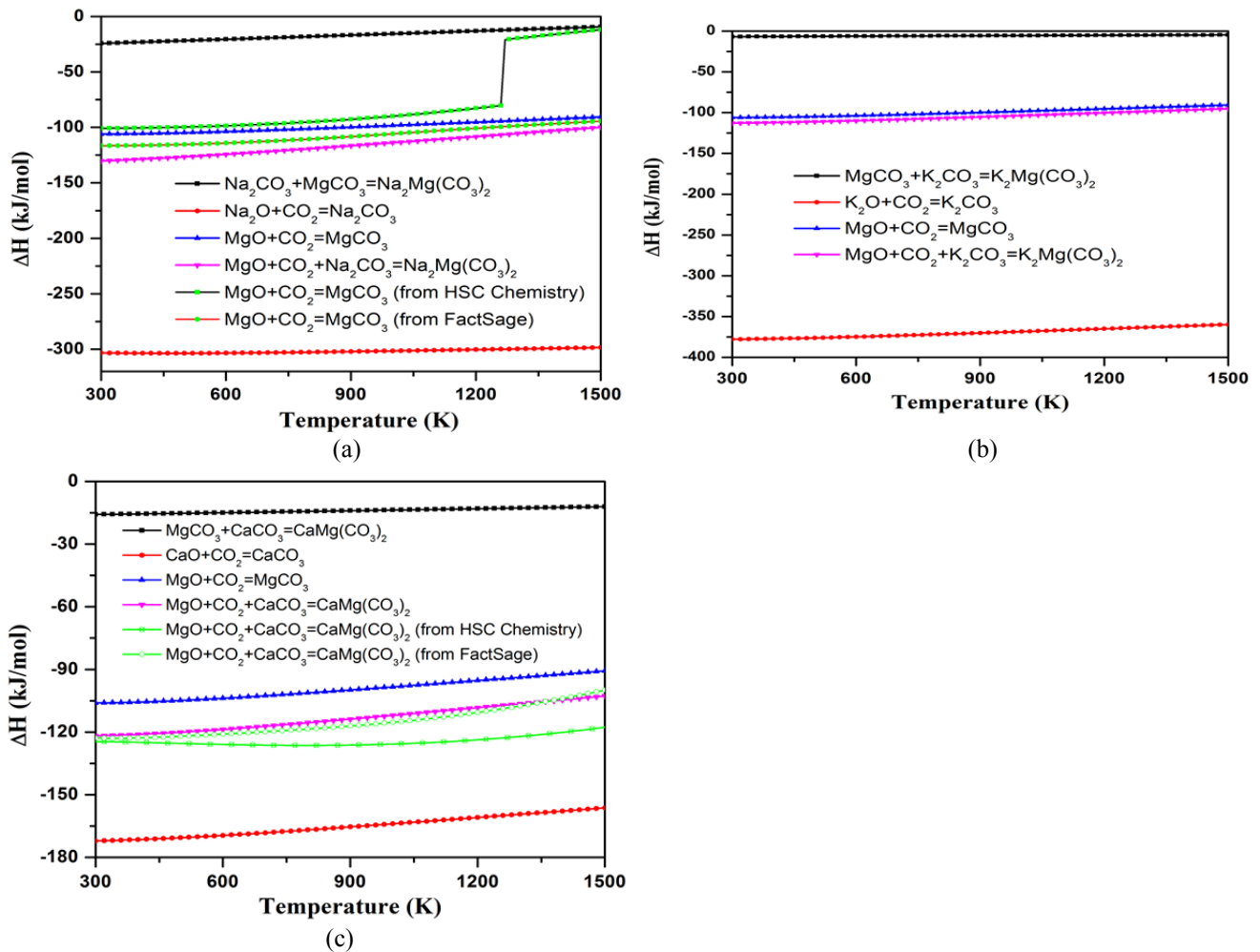


Fig. 2. The calculated heats of reactions (ΔH) of the CO_2 capture reactions versus temperatures. (a) Na_2CO_3 -promoted MgO ; (b) K_2CO_3 -promoted MgO ; (c) CaCO_3 -promoted MgO .

system shown in Fig. 2(c). However, as shown in Fig. 2(b), the ΔH of reaction $\text{MgO} + \text{CO}_2 + \text{K}_2\text{CO}_3 = \text{K}_2\text{Mg}(\text{CO}_3)_2$ is close to that of $\text{MgO} + \text{CO}_2 = \text{MgCO}_3$.

From the Gibbs free energy change (ΔG) of the CO_2 capture reaction (Fig. 3), when $\Delta G = 0$, we can obtain the turnover temperature (T_t listed in Table 3) above which the reverse reaction starts to release CO_2 . From Fig. 3(a), one can see that for the reaction $\text{MgO} + \text{CO}_2 = \text{MgCO}_3$, its T_t from HSC Chemistry (575 K) and FactSage (670 K) databases has about 95 K (ΔT in Fig. 3(a)) difference while our calculated value (590 K) is closer to the value obtained from HSC Chemistry database. Within the temperature range, the ΔG (T) of reaction $\text{MgO} + \text{CO}_2 + \text{Na}_2\text{CO}_3 = \text{Na}_2\text{Mg}(\text{CO}_3)_2$ ($T_t = 795$ K) is lower than that of $\text{MgO} + \text{CO}_2 = \text{MgCO}_3$ ($T_t = 660$ K), but is higher than that of $\text{Na}_2\text{O} + \text{CO}_2 = \text{Na}_2\text{CO}_3$ reaction ($T_t > 1500$ K).

For the reaction of $\text{MgO} + \text{CaCO}_3$ capturing CO_2 to form dolomite as shown in Fig. 3(c), our calculated ΔG is in good agreement with the data from both HSC Chemistry and FactSage databases. The T_t of $\text{MgO} + \text{CO}_2 + \text{CaCO}_3 = \text{CaMg}(\text{CO}_3)_2$ ($T_t = 660$ K) is higher than that of $\text{MgO} + \text{CO}_2 = \text{MgCO}_3$ ($T_t = 590$ K), but lower than that of the $\text{CaO} + \text{CO}_2 = \text{CaCO}_3$ reaction ($T_t = 1095$ K). Similar results also

can be found for the $\text{MgO} + \text{K}_2\text{CO}_3$ sorbent system as shown in Fig. 3(b). As opposed to the $\text{MgO} + \text{Na}_2\text{CO}_3$ and $\text{MgO} + \text{CaCO}_3$ sorbents, the calculated ΔG (T) of reaction $\text{MgO} + \text{CO}_2 + \text{K}_2\text{CO}_3 = \text{K}_2\text{Mg}(\text{CO}_3)_2$ is only slightly lower than that of $\text{MgO} + \text{CO}_2 = \text{MgCO}_3$. As a result their T_t differ by only 10 K.

Application to Pre- and Post-Combustion CO_2 Capture Technologies

According to Eq. (1), we can examine the relationships among the chemical potential ($\Delta\mu(T, P)$), the temperature (T), and the CO_2 pressure (P_{CO_2}) of the CO_2 capture reactions by the carbonates-promoted MgO sorbents. Fig. 4 shows the corresponding results where only the contourgram of $\Delta\mu(T, P) = 0$ curve is plotted explicitly. The lines in the figure show the values of T and P where $\Delta\mu(T, P) = 0$ for each reaction. Around each line is a good region for absorption and desorption with optimal conditions because of the minimal energy costs at the respective temperature and pressure conditions. Above the lines, $\Delta\mu(T, P) < 0$, the respective reactions are driven in the CO_2 absorption direction and the double salts are formed, while below the respective lines, $\Delta\mu(T, P) > 0$, the reactions are driven in

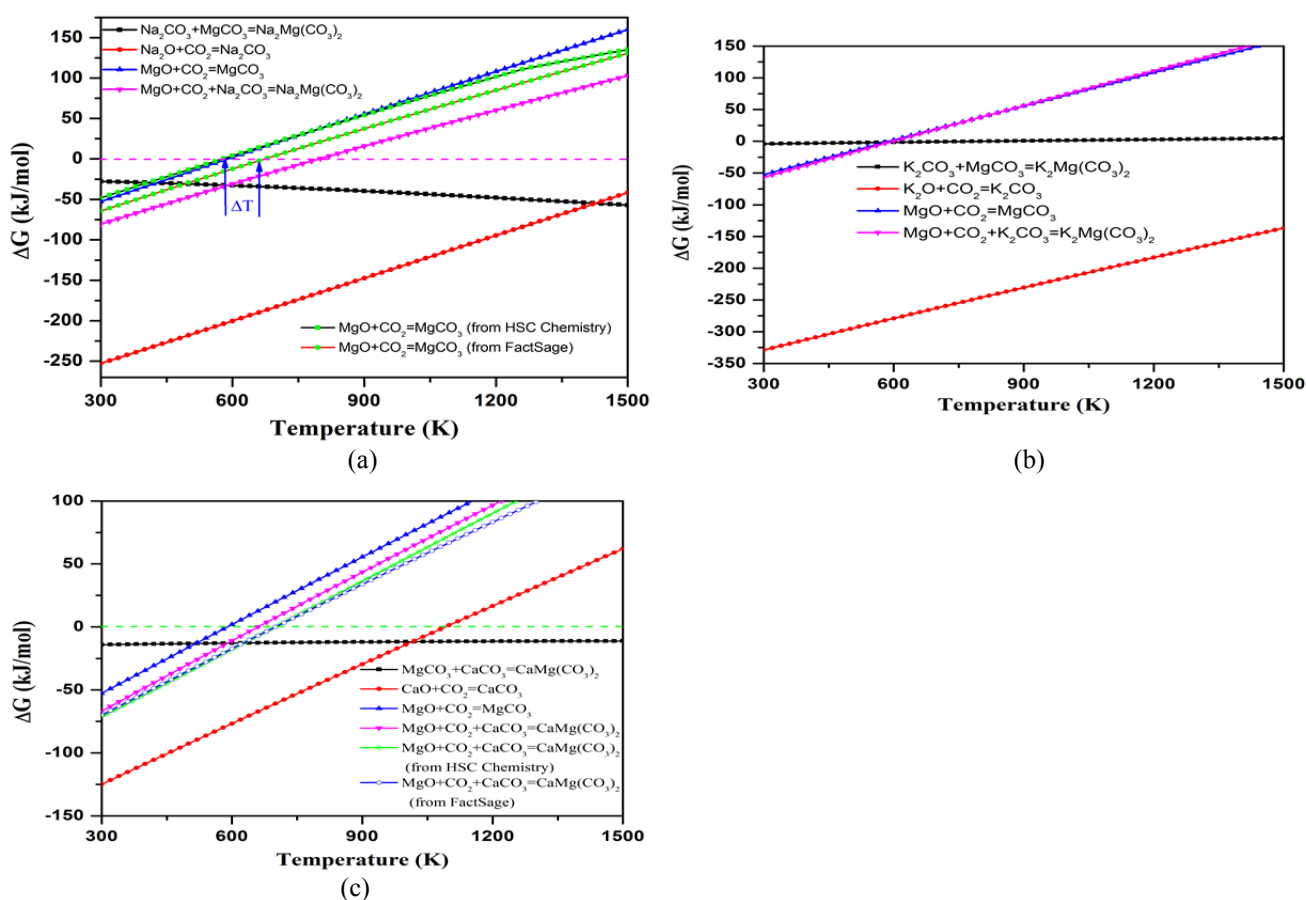


Fig. 3. The calculated Gibbs free energy changes of the CO₂ capture reactions. (a) Na₂CO₃-promoted MgO; (b) K₂CO₃-promoted MgO; (c) CaCO₃-promoted MgO.

the opposite direction, releasing CO₂ and regenerating the MgO and carbonates.

As aforementioned and shown in Fig. 4, all of the reactions are thermodynamically favorable over a certain range of temperatures and P_{CO₂}, which means that under such conditions CO₂ is thermodynamically favored to be captured by these carbonate-promoted MgO mixtures.

The operating conditions for absorption/desorption processes depend on the specific pre- and post-combustion technologies. Under pre-combustion conditions, after water-gas shift, the gas stream mainly contains CO₂, H₂O and H₂. The partial CO₂ pressure is around 10–20 bar and the temperature is around 523–773K for warm gas clean-up. To minimize the energy consumption, the ideal sorbents should work in these pressure and temperature ranges to separate CO₂ from H₂. The separated H₂ can be used for fuel cell power production or for IGCC applications (Zhang *et al.*, 2013). We define T_1 for each reaction to be the temperature at which the $\Delta\mu(P, T) = 0$ curve crosses the P_{CO₂} = 10 bar line in Fig. 4. This temperature T_1 , listed in Table 3, is the temperature above which the sorbent cannot absorb CO₂ and will release CO₂. This indicates that, during capture of CO₂, the operating temperature should be lower than T_1 , whereas the operating temperature must be higher than T_1 in order to release CO₂. For post-combustion conditions, the gas stream mainly contains CO₂ and N₂, the

partial pressure of CO₂ is around 0.1–0.2 bar (typically 0.14 bar), and the temperature range is significantly lower. We similarly define T_2 to be the temperature at which the $\Delta\mu = 0$ curve for each reaction crosses the horizontal P = 0.1 bar line in Fig. 4. These corresponding T_2 values obtained for post-combustion capture by these three carbonate-promoted MgO sorbents are also listed in Table 3.

It should be pointed out that the T_1 and T_2 values listed in Table 3 are the highest temperatures at which the CO₂ absorption reaction still can occur for the specific pre- and post-combustion conditions. However, depending on which capture technology is considered, the real capture temperatures should be lower than that shown in Table 3 (T_1 and T_2). The United States Department of Energy programmatic goal for post-combustion CO₂ capture is to capture at least 90% CO₂ with an increase cost in electricity of no more than 35%, whereas in the case of pre-combustion CO₂ capture it is to capture at least 90% CO₂ with an increase cost in electricity of no more than 10% (DOE-NETL, 2007). Assuming that 90% of the CO₂ is captured, for a worst case (such as in a single-stage fluidized bed), the final CO₂ partial pressure will be lower than its initial value at 0.01–0.02 bar for post-combustion and at 1–2 bar for pre-combustion. Therefore, at the end, the final T_1 and T_2 must shift to a lower temperature range. Generally, at high temperature the kinetics of the CO₂ capture reaction

Table 2. The CO₂ capture capacities in weight percentage (wt%), the calculated energy changes and thermodynamic properties of CO₂ capture reactions by solids. Enthalpies and Gibbs free energies correspond to partial pressures of CO₂ of 1 bar. (unit: kJ/mol).

Reactions	CO ₂ wt%	ΔE^{DFT}	ΔE^{ZP}	$\Delta H(T = 300 \text{ K})$	$\Delta G(T = 300 \text{ K})$
MgO + CO ₂ = MgCO ₃	109.19	-92.51	8.71	-106.05 -100.89 ^a -116.67 ^b	-52.67 -48.21 ^a -64.20 ^b
MgO + Na ₂ CO ₃ + CO ₂ = Na ₂ Mg(CO ₃) ₂	30.14	-120.21	9.92	-130.38	-80.57
MgO + K ₂ CO ₃ + CO ₂ = K ₂ Mg(CO ₃) ₂	24.65	-99.01	9.07	-113.01	-56.83
MgO + CaCO ₃ + CO ₂ = CaMg(CO ₃) ₂	31.34	-109.31	9.68	-121.88 -124.60 ^a -122.92 ^b	-66.85 -71.44 ^a -69.92 ^b
CaO + CO ₂ = CaCO ₃	78.48	-161.75	5.52	-176.75 -178.17 ^a -179.16 ^b	-129.53 -130.13 ^a -131.04 ^b
Na ₂ O + CO ₂ = Na ₂ CO ₃	71.01	-284.71	4.59	-282.37	-231.90
K ₂ O + CO ₂ = K ₂ CO ₃	46.72	-363.42	5.87	-359.31	-309.50
MgCO ₃ + Na ₂ CO ₃ = Na ₂ Mg(CO ₃) ₂		-27.70	1.22	-24.33	-27.90
MgCO ₃ + K ₂ CO ₃ = K ₂ Mg(CO ₃) ₂		-6.50	0.36	-6.96	-4.16
MgCO ₃ + CaCO ₃ = CaMg(CO ₃) ₂		-16.80	0.97	-15.83 -23.71 ^a -6.25 ^b	-14.19 -23.23 ^a -5.72 ^b

^a Calculated by the HSC Chemistry package.^b Calculated by the FactSage package.**Table 3.** The turnover temperature (T_1) at $P_{\text{CO}_2} = 1$ bar, the highest temperatures for sorbents capturing CO₂ at pre-combustion (T_1) condition with $P_{\text{CO}_2} = 10$ bar and post-combustion (T_2) condition with $P_{\text{CO}_2} = 0.1$ bar.

Reactions	T_1	Pre-combustion	Post-combustion
	(K)	T_1 (K)	T_2 (K)
MgO + Na ₂ CO ₃ + CO ₂ = Na ₂ Mg(CO ₃) ₂	795	915	710
MgO + K ₂ CO ₃ + CO ₂ = K ₂ Mg(CO ₃) ₂	600	665	545
MgO + CaCO ₃ + CO ₂ = CaMg(CO ₃) ₂	660	740	600
	695 ^a , 705 ^b	785 ^a , 790 ^b	635 ^a , 630 ^b
MgO + CO ₂ = MgCO ₃	590	600	535
	575 ^a , 675 ^b	655 ^a , 760 ^b	520 ^a , 605 ^b
CaO + CO ₂ = CaCO ₃	1095	1245	975
	1155 ^a , 1165 ^b	1340 ^a , 1345 ^b	1025 ^a , 1030 ^b
Na ₂ O + CO ₂ = Na ₂ CO ₃	hT ^c	hT	hT
K ₂ O + CO ₂ = K ₂ CO ₃	hT	hT	hT

^a Calculated by the HSC Chemistry package.^b Calculated by the FactSage package.^c hT means the maximum temperature exceeds our temperature range (1500 K).

are faster. From the kinetics point of view, the capture temperature should be as close to the corresponding T_1 and T_2 as possible.

However, as a CO₂ solid sorbent, the materials of interest should not only be able to absorb CO₂ easily, but also easily release the CO₂ from the products. As shown in Figs. 3 and 4, to reverse the CO₂ capture reactions (a) and (b), energy input is needed as these reverse reactions are endothermic. The operating temperature for CO₂ desorption should be higher than the indicated temperatures T_1 (pre-combustion) or T_2 (post-combustion) as shown in Fig. 4. From Table 3 and Fig. 4, one can see that the maximum capture temperatures (T_1 , T_2) have the following trend: Na₂CO₃ + MgO > K₂CO₃ + MgO > CaCO₃ + MgO.

Obviously, compared to pure MgO, when add carbonates (Na₂CO₃, K₂CO₃ and CaCO₃) into MgO, the corresponding T_1 and T_2 increase.

Based on the results shown in Fig. 4 and Table 3, when we mix MgO with carbonate (M₂CO₃ (M = Na, K), CaCO₃) or oxide (M₂O and CaO, which is present in the carbonate form after first cycle), the T_1 and T_2 of CO₂ capture reactions by the mixed systems are located between those of MgO and the corresponding oxide (Na₂O, K₂O, CaO). As shown in Fig. 4(a), our calculated P-T ($\Delta\mu = 0$) relationship of MgO capture CO₂ reaction is in good agreement with the data derived from HSC Chemistry database, but has a significant discrepancy with the data from FactSage database. As listed in Table 3, the T_1 and T_2 of MgO + CO₂ = MgCO₃

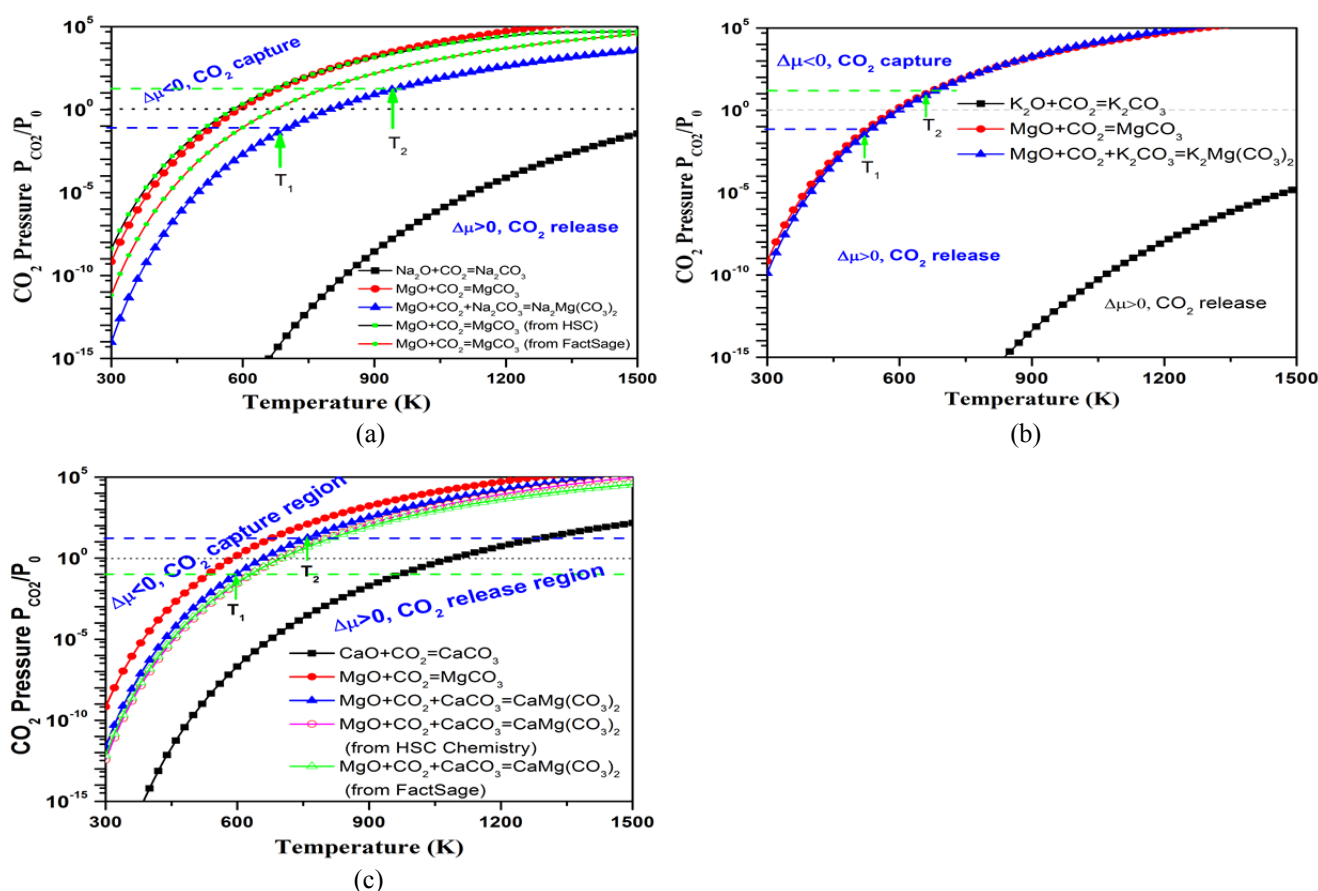


Fig. 4. Contour plots of the calculated chemical potential ($\Delta\mu$) versus temperature and the CO₂ pressure (P plotted in logarithmic scale) for the CO₂ capture reactions. Only $\Delta\mu = 0$ curve is shown explicitly. For each reaction, above its $\Delta\mu = 0$ curve, their $\Delta\mu < 0$, which means the sorbents absorb CO₂ and the reaction goes forward, whereas below the $\Delta\mu = 0$ curve, their $\Delta\mu > 0$, which indicates CO₂ start to be released and reaction reverses with regeneration of the sorbents. (a) Na₂CO₃-promoted MgO; (b) K₂CO₃-promoted MgO; (c) CaCO₃-promoted MgO.

reaction are 660 K and 535 K, respectively. When Na₂CO₃ (or Na₂O) is mixed into MgO, by forming Na₂Mg(CO₃)₂ double salt, the corresponding T_1 and T_2 of the mixed sorbent increase to 915 K and 710 K, respectively. Obviously, as seeing in Fig. 4(a), the P-T ($\Delta\mu = 0$) relationship of MgO + Na₂CO₃ capture CO₂ is between those of pure MgO and Na₂O.

Similar conclusions can be drawn for the cases of MgO + K₂CO₃ and MgO + CaCO₃ shown in Figs. 4(b) and 4(c). As listed in Table 3, compared to pure MgO, the MgO + K₂CO₃ mixture only has about 10 K increase on its T_1 and T_2 values, which indicates that adding K₂CO₃ (or K₂O) does not increase the maximum CO₂ capture temperature much, but could affect its CO₂ capture capacity and kinetics as demonstrated experimentally in the literatures (Lee *et al.*, 2006, 2008; Xiao *et al.*, 2011). As we know that another potential advantage of mixing solids is to gain entropy and to increase the surface area of active part of the solid for having faster reaction rate. The K₂CO₃ + MgO sorbent doesn't show too much advantage in shifting the capture temperature, but may enhance the kinetics of the capture process and eventually make the mixtures more efficient. In the case of MgO + CaCO₃, as shown in Fig. 4(c) and Table

3, our calculated P-T relationship is in good agreement with the data derived from both HSC Chemistry and FactSage databases. Compared to pure MgO, MgO + CaCO₃ also increase the T_1 and T_2 up to 740 K and 600 K respectively, which perfectly fits the desired operating temperature range of the warm gas clean up technology, and therefore, it can be used as CO₂ sorbent in pre-combustion technology.

As one can see from Figs. 2 and 4, compared to pure MgO, the Na₂O, K₂O and CaO have stronger interaction with CO₂ and have higher T_1 and T_2 values. Adding these "strong" CO₂ sorbent into relatively "weak" MgO sorbent, the thermodynamic behaviors of the mixed sorbent are usually located between those of strong and weak sorbents. Similar concepts were applied to decrease the CO₂ capture temperature of the "strong" sorbent which acts as the effective CO₂ capture component while the "weak" part acts as a stabilizer to lift reaction free energy up (less negative), such as the Li₂O + SiO₂ and Li₂O + ZrO₂ systems (Duan, 2013; Duan *et al.*, 2013). In this study, however, we use the "weak" MgO as the active capture component and want to increase its CO₂ capture temperature, the "strong" part (Na₂CO₃, K₂CO₃, CaCO₃) involved in the formation of double salt to bring thermodynamic properties (ΔH and

ΔG) of mixed system more negative, and in turn, increase the maximum CO₂ capture temperatures T_1 and T_2 . Such results indicate that by adding other solids, we can improve operating conditions of the existing sorbent and synthesize new sorbent which could work at the desired operating temperature range.

CONCLUSIONS

First-principles density functional theory combined with phonon density of states calculations have been employed to obtain the thermodynamic properties of double salts M₂Mg(CO₃)₂ (M = Na, K) and CaMg(CO₃)₂. Based on the calculated thermodynamic data, their CO₂ capture properties were fully investigated.

Although pure MgO has a very high theoretical CO₂ capture capacity (109.2 wt%), its practical CO₂ capture performance at medium temperature range is poor and its maximum capture temperature (590 K when P_{CO₂} = 1 bar, see Table 3) is located in the lower end of the desired temperature range of 523–773 K for warm gas clean up technology. This study proved that adding another oxide or carbonate could increase its capture temperature and in turn may improve its practical capture capacity. Our calculated results showed that by mixing alkali metal oxides (M₂O (M = Na, K), CaO) or carbonates (M₂CO₃ (M = Na, K), CaCO₃) into MgO, the corresponding mixed systems have higher CO₂ capture temperatures through the reactions MgO + CO₂ + M₂CO₃ = M₂Mg(CO₃)₂ and MgO + CO₂ + CaCO₃ = CaMg(CO₃)₂ respectively. Under pre-combustion conditions with P_{CO₂} = 10 bar, the Na₂CO₃-, K₂CO₃- and CaCO₃-promoted MgO sorbents can capture CO₂ up to 915 K, 665 K and 740 K respectively. While under post-combustion conditions with P_{CO₂} = 0.1 bar, their maximum CO₂ capture temperatures are 710 K, 545 K and 600 K respectively. Among them, Na₂CO₃- and CaCO₃-promoted MgO sorbents have large effects on increasing CO₂ capture temperatures.

Our results indicated that by mixing carbonates into MgO, it is possible to shift its CO₂ capture temperature to higher range to fit the practical industrial needs. These results provide some general guidelines to design and synthesize new CO₂ sorbents and in such cases computational modeling can play a decisive role for identifying materials with optimal performance.

ACKNOWLEDGMENTS

One of us (YD) thanks Drs. G. Richards, D. Luebke and D. C. Sorescu for fruitful discussions.

REFERENCES

Abbasi, E., Hassanzadeh, A. and Abbasian, J. (2013). Regenerable MgO-based Sorbent for High Temperature CO₂ Removal from Syngas: 2. Two-zone Variable Diffusivity Shrinking Core Model with Expanding Product Layer. *Fuel* 105: 128–134.

Allen, M.R., Frame, D.J., Huntingford, C., Jones, C.D., Lowe, J.A., Meinshausen, M. and Meinshausen, N. (2009).

Warming Caused by Cumulative Carbon Emissions Towards the Trillionth Tonne. *Nature* 458: 1163–1166.

DOE-NETL (2007). Cost and Performance Baseline for Fossil Energy Plants, Volume 1: Bituminous Coal and Natural Gas to Electricity Final Report, http://www.netl.doe.gov/energy-analyses/baseline_studies.html.

Duan, Y. and Sorescu, D.C. (2009). Density Functional Theory Studies of the Structural, Electronic, and Phonon Properties of Li₂O and Li₂CO₃: Application to CO₂ Capture Reaction. *Phys. Rev. B* 79: 014301.

Duan, Y. and Sorescu, D.C. (2010). CO₂ Capture Properties of Alkaline Earth Metal Oxides And Hydroxides: A Combined Density Functional Theory and Lattice Phonon Dynamics Study. *J. Chem. Phys.* 133: 074508.

Duan, Y. (2011). Electronic Structural and Electrochemical Properties of Lithium Zirconates and Their Capabilities of CO₂ Capture: A First-principles Density-functional Theory and Phonon Dynamics Approach. *J. Renewable Sustainable Energy* 3: 013102.

Duan, Y., Zhang, B., Sorescu, D.C. and Johnson, J.K. (2011). CO₂ Capture Properties of M-C-O-H (M = Li, Na, K) Systems: A Combined Density Functional Theory and Lattice Phonon Dynamics Study. *J. Solid State Chem.* 184: 304–311.

Duan, Y. (2012). A First-principles Density Functional Theory Study of the Electronic Structural and Thermodynamic Properties of M₂ZrO₃ and M₂CO₃ (M = Na, K) and Their Capabilities Of CO₂ Capture. *J. Renewable Sustainable Energy* 4: 013109.

Duan, Y., Luebke, D. and Pennline, H.W. (2012). Efficient Theoretical Screening of Solid Sorbents for CO₂ Capture Applications. *Int. J. Clean Coal Energy* 1: 1–11.

Duan, Y. (2013). Structural and Electronic Properties of Li₃ZrO₆ and Its CO₂ Capture Capabilities: An *ab initio* Thermodynamic Approach. *Phys. Chem. Chem. Phys.* 15: 9752–9760.

Duan, Y., Pfeiffer, H., Li, B.Y., Romero-Ibarra, I.C., Sorescu, D.C., Luebke, D. and Halley, J.W. (2013). CO₂ Capture Properties of Lithium Silicates with Different Ratios of Li₂O/SiO₂: An *ab initio* Thermodynamic and Experimental Approach. *Phys. Chem. Chem. Phys.* 15: 13538–13558.

Hassanzadeh, A. and Abbasian, J. (2010). Regenerable MgO-based Sorbents for High-temperature CO₂ Removal from Syngas: 1. Sorbent Development, Evaluation, and Reaction Modeling. *Fuel* 89: 1287–1297.

Haszeldine, R.S. (2009). Carbon Capture and Storage: How Green Can Black Be? *Science* 325: 1647–1652.

Hesse, K.F. and Simons, B. (1982). Crystal-structure of Synthetic K₂Mg(CO₃)₂. *Z. Kristallogr.* 161: 289–292.

Kresse, G. and Hafner, J. (1993). *Abinitio* Molecular-Dynamics for Liquid-Metals. *Phys. Rev. B* 47: 558–561.

Lee, S.C., Choi, B.Y., Lee, T.J., Ryu, C.K., Soo, Y.S. and Kim, J.C. (2006). CO₂ Absorption and Regeneration of Alkali Metal-based Solid Sorbents. *Catal. Today* 111: 385–390.

Lee, S.C. and Kim, J.C. (2007). Dry Potassium-based Sorbents for CO₂ Capture. *Catal. Surv. Asia* 11: 171–185.

Lee, S.C., Chae, H.J., Lee, S.J., Choi, B.Y., Yi, C.K., Lee,

- J.B., Ryu, C.K. and Kim, J.C. (2008). Development of Regenerable MgO-based Sorbent Promoted with K_2CO_3 for CO_2 Capture at Low Temperatures. *Environ. Sci. Technol.* 42: 2736–2741.
- Li, B.Y., Duan, Y., Luebke, D. and Morreale, B. (2013). Advances in CO_2 Capture Technology: A Patent Review. *Appl. Energy* 102: 1439–1447.
- Li, Y.J., Zhao, C.S., Duan, L.B., Liang, C., Li, Q.Z., Zhou, W. and Chen, H.C. (2008). Cyclic Calcination/Carbonation Looping Of Dolomite Modified with Acetic Acid for CO_2 Capture. *Fuel Process. Technol.* 89: 1461–1469.
- Lund, H. and Mathiesen, B.V. (2009). Energy System Analysis of 100% Renewable Energy Systems-The Case of Denmark in Years 2030 and 2050. *Energy* 34: 524–531.
- MacDowell, N., Florin, N., Buchard, A., Hallett, J., Galindo, A., Jackson, G., Adjiman, C.S., Williams, C.K., Shah, N. and Fennell, P. (2010). An Overview of CO_2 Capture Technologies. *Energy Environ. Sci.* 3: 1645–1669.
- Markewitz, P., Kuckshinrichs, W., Leitner, W., Linssen, J., Zapp, P., Bongartz, R., Schreiber, A. and Muller, T.E. (2012). Worldwide Innovations in the Development of Carbon Capture Technologies and the Utilization of CO_2 . *Energy Environ. Sci.* 5: 7281–7305.
- Mayorga, S.G., Weigel, S.J., Gaffney, T.R. and Brzozowski, J.R. (2001). Carbon Dioxide Adsorbents Containing Magnesium Oxide Suitable for Use at High Temperatures, USA Patent, No. 6280503B1
- Monkhorst, H.J. and Pack, J.D. (1976). Special Points for Brillouin-Zone Integrations. *Phys. Rev. B* 13: 5188–5192.
- Montero, J.M., Wilson, K. and Lee, A.F. (2010). Cs Promoted Triglyceride Transesterification over MgO Nanocatalysts. *Topics in Catalysis* 53: 737–745.
- Pabst, A., (1973). Crystallography and Structure of Eitelite, $Na_2Mg(CO_3)_2$. *Am. Mineral.* 58: 211–217.
- Parlinski, K., Li, Z.Q. and Kawazoe, Y. (1997). First-principles Determination of the Soft Mode in Cubic ZrO_2 . *Phys. Rev. Lett.* 78: 4063–4066.
- Parlinski, K., (2010). Software PHONON.
- Perdew, J.P. and Wang, Y. (1992). Accurate and Simple Analytic Representation of the Electron-Gas Correlation-Energy. *Phys. Rev. B* 45: 13244–13249.
- Reeder, R.J. and Markgraf, S.A. (1986). High-temperature Crystal-chemistry of Dolomite. *Am. Mineral.* 71: 795–804.
- Siriwardane, R., Poston, J., Chaudhari, K., Zinn, A., Simonyi, T. and Robinson, C. (2007). Chemical-looping Combustion of Simulated Synthesis Gas Using Nickel Oxide Oxygen Carrier Supported on Bentonite. *Energy Fuels* 21: 1582–1591.
- Stammore, B.R. and Gilot, P. (2005). Review-calcination and Carbonation of Limestone during Thermal Cycling for CO_2 Sequestration. *Fuel Process. Technol.* 86: 1707–1743.
- Wang, Q., Luo, J., Zhong, Z. and Borgna, A. (2011). CO_2 Capture by Solid Adsorbents and Their Applications: Current Status and New Trends. *Energy Environ. Sci.* 4: 42–55.
- White, C.M., Strazisar, B.R., Granite, E.J., Hoffman, J.S. and Pennline, H.W. (2003). Separation and Capture of CO_2 from Large Stationary Sources and Sequestration in Geological Formations-coalbeds and Deep Saline Aquifers. *J. Air Waste Manage. Assoc.* 53: 645–715.
- Xiao, G.K., Singh, R., Chaffee, A. and Webley, P. (2011). Advanced Adsorbents Based on MgO and K_2CO_3 for Capture of CO_2 at Elevated Temperatures. *Int. J. Greenhouse Gas Control* 5: 634–639.
- Yang, Y.P., Zhai, R.R., Duan, L.Q., Kavosh, M., Patchigolla, K. and Oakey, J. (2010). Integration and Evaluation of a Power Plant with a CaO-based CO_2 Capture System. *Int. J. Greenhouse Gas Control* 4: 603–612.
- Zhang, K., Li, X.S., Duan, Y., Singh, P., King, D.L. and Li, L. (2013). Roles of Double Salt Formation and $NaNO_3$ in Na_2CO_3 -promoted MgO Sorbent for Intermediate Temperature CO_2 Removal. *Int. J. Greenhouse Gas Control* 12: 351–358.

Received for review, May 30, 2013

Accepted, July 11, 2013